

Integral field spectroscopy of the nearby spiral galaxy NGC 5668

R. A. Marino^{1,2}, A. Gil de Paz¹, A. Castillo-Morales¹, J. C. Muñoz-Mateos¹, and S. F. Sánchez²

¹ Departamento de Astrofísica y CC. de la Atmósfera, Universidad Complutense de Madrid, Madrid 28040, Spain

² Centro Astronómico Hispano Alemán, Calar Alto, CSIC-MPG, C/Jesús Durbán Remón 2-2, E-04004 Almeria, Spain

Abstract

We analyze the full bi-dimensional spectral cube of the nearby spiral galaxy NGC 5668, which was obtained as a mosaic of 6 pointings, covering a total area of 2×3 arcmin², obtained with the PPAK Integral Field Unit at the Calar Alto (CAHA) observatory 3.5 m telescope. From these data we the bidimensional spatial distribution maps of the attenuation of the ionized gas (from the $H\alpha/H\beta$ Balmer decrement), and chemical abundances of oxygen (using strong line methods such as the R_{23}). In addition to these maps, we also extract the spectra of individual HII regions by adding the flux over several PPAK fibers to increase the signal-to-noise ratio of the spectra and reduce the uncertainties in the properties derived. The spectra of these regions are compared with the predictions of evolutionary synthesis models for evolved stellar populations. Both the measurements of spectroscopic indices and the full spectra will be used. Finally, given that most of the properties of the stars, gas, and dust in galaxies vary with radius the spectra of concentric annuli are also extracted and analyzed.

1 Introduction

The formation and evolution of galactic disks remain two of the most important aspects in extragalactic astronomy. Despite significant progress in the recent past regarding our understanding of the history of both the thick and thin disks, important questions remain unanswered: How old are the disks seen in the spiral galaxies today? How did they chemically evolve? Are they growing inside-out, as proposed to explain the color and metallicity gradients in our own Milky Way? Do they have an edge? How efficient is the stellar radial diffusion? Until recently the study of the properties of spiral disks has been limited to broad-band

imaging data and/or long-slit spectroscopy, which has severely limited the reach of previous works [14, 17]. Our effort is committed to add another dimension to the study of nearby spiral galaxies thanks to the use of wide-field integral-field spectrometers. We have recently started a project to map a sample of a dozen nearby galaxies using mosaics obtained with the two largest IFU available to date: PPAK at the CAHA 3.5 m and VIMOS at ESO-VLT. In particular, these unprecedented sets of data have allowed us to get insights the properties of dust and star formation in galaxies. In this work we present the pilot study of the full bi-dimensional spectral cube of the nearby spiral galaxy NGC 5668, (see Fig. 1), which was obtained as a mosaic of 6 pointings by using the PPAK Integral Field Unit at the Calar Alto (CAHA) observatory 3.5 m telescope. Despite the relatively modest collecting area of the CAHA 3.5 m telescope, the broad spectral coverage (from 3700 to 7000 Å) and relatively good spectral resolution ($R = 500$) of PPAK make of this instrument the best tool for study stellar populations, dust content, and physical conditions of the gas (temperature, density, chemical abundances) in spatially resolved galaxies.

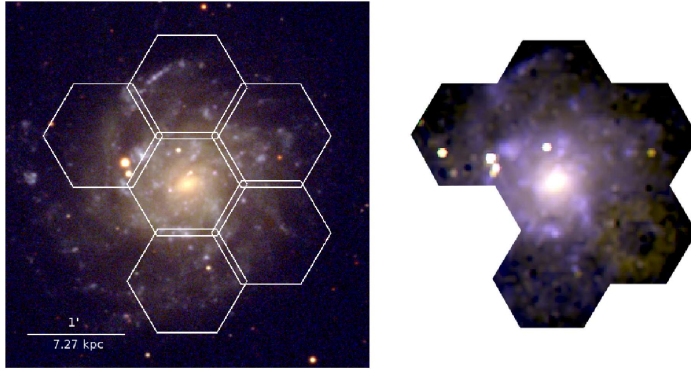


Figure 1: *Left*: False-color SDSS optical image (from 4458 to 7706 Å) of NGC 5668 centered at RA(2000) $14^{\text{h}}33^{\text{m}}24.3^{\text{s}}$ and DEC(2000) $+04^{\circ}33'24.3''$. North is down and east is to the right. Plate scale is 0.396 arcsec/pix. *Right*: Synthetic false-color image obtained from the PPAK datacube and the response curves of the SDSS u,g and r filters. Center and orientation are the same as in the left panel. Plate scale is 1 arcsec/pix in this case.

2 The case of NGC 5668

NGC 5668 is a nearly face-on late-type spiral galaxy, that is classified as a Sc(s)II–III type on the Hubble sequence. There is a weak bar or oval inner structure $12''$ in size visible on the image, reflected by a small shoulder in the surface brightness profile published by [19]. The outer disk (beyond $R < 100''$) is slightly asymmetric and more extended towards the North. For this work we adopted a distance of 25 Mpc, $(m - M) = 31.99$ mag, assuming a cosmology with $H_0 = 73 \text{ km s}^{-1} \text{ Mpc}^{-1}$, $\Omega_{\text{matter}} = 0.27$, $\Omega_{\text{vacuum}} = 0.73$, NED¹. NGC 5668 has been also recently observed by a number of facilities, including SAURON at the WHT,

¹NASA/IPAC Extragalactic Database, <http://nedwww.ipac.caltech.edu/>

SDSS, Spitzer and the Medium-deep Imaging Survey of GALEX. This galaxy is also classified as a “supernova factory” due to the discovery of several supernova explosions in recent epoch [11]. This dataset in combination with the PPAK mosaic (focus of this work) should allow the most extensive analysis to date of the ionized-gas and stellar population properties in this galaxy.

3 Observation and data reduction

We have observed the nearly face-on spiral galaxy NGC 5668 with the PPAK (Pmas fiber PAck) IFU of PMAS, the Potsdam Multi-Aperture Spectrophotometer, at the Calar Alto (CAHA, Spain) observatory 3.5 m telescope. The observations were carried out on June 22-23-24, 2007. We used the PPAK mode that yields a total field-of view (FoV) of $74'' \times 65''$ (hexagonal packed) for each pointing, covering a total area of roughly 2×3 arcmin² (we obtained a mosaic of 6 PPAK pointings in order to study this relatively extended object). The final mosaic includes a total of 2292 raw-spectra, with 1982 science spectra that cover the broad spectral range 3700-7131 Å. The reduction procedure applied for NGC 5668 follows the techniques and sequence described in [18]. The reduction was carried out using R3D, a software package for reducing fiber-based spectroscopic data focused on the reduction of IFS of IFUs.

4 Analysis

The data were analyzed using tasks including in different packages in IRAF². Furthermore we have used own software based on IDL, Interactive Data Language, to analyze the spectra where the feature in the continuum are clearly visible. We analyzed the map of H α emission, the brightest line in the optical spectrum of HII regions under most physical conditions and selected 73 HII regions in the galaxy. We also generated continuum-subtracted maps of the strongest emission lines (besides H α): [OII] λ 3727; [OIII] $\lambda\lambda$ 4959, 5007; H β ; [NII] λ 6548; [NII] λ 6583, λ 6548 and [SII] λ 6717, λ 6731. To investigate the radial variation of the physical properties in the galaxy and the possible presence of rings of SF (such as in many early to intermediate Hubble types), we also selected 18 concentric annuli, starting from the center of the image (defined as the peak of the optical continuum emission), and continuing with the other annuli at increments of $5''$ in radius until reaching the outermost ring at $R_{\text{FINAL}} = 95''$.

5 Results

Many important topics in astrophysics involve the physics of ionized gases and the interpretation of their emission line spectra. The distribution of HII regions is an excellent tracer of

²IRAF is distributed by the National Optical Astronomy Observatories, which are operated by the Association of Universities for Research in Astronomy, Inc., under cooperative agreement with the National Science Foundation.

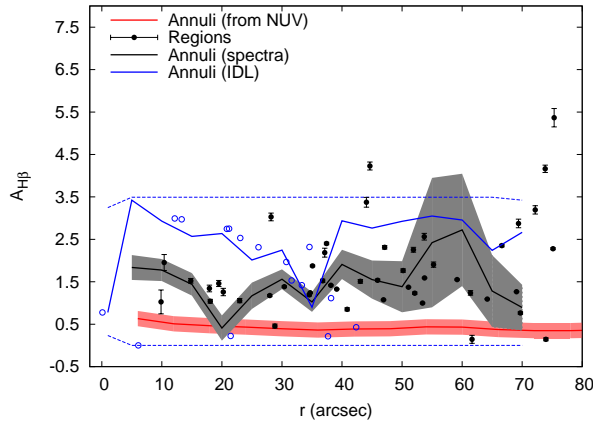


Figure 2: Representation of radial variation of the dust attenuation. Filled circles represent the values obtained from individual HII regions based on the Balmer decrement. The black line represents Balmer decrement data for the concentric annuli. The red line is the attenuation trend calculated from the slope of the UV continuum (or, equivalently, the FUV–NUV color). The blue line show the attenuation that we find for the stellar continuum at optical wavelengths with our IDL fitting routine.

recent massive star formation in spiral galaxies and spectra can reveal details surrounding the first generations of star birth and the formation of the heavy elements in the young universe.

5.1 Attenuation

We utilized three different methods to estimate the attenuation. For the stellar continuum we utilized the UV data available on NGC 5668. Whereas for gas attenuation we utilized the Balmer decrements in both individual HII regions and the concentric annuli. Under Case B conditions with temperatures ~ 10000 K and electron densities ~ 100 cm^{-3} , (in our case we find N_e of 190 cm^{-3} for the regions) the theoretical $\text{H}\alpha/\text{H}\beta$ ratio should be close to 2.86 [12]. The last method that we have employed is based in the determination of the continuum extinction in the concentric annuli spectra derived by our IDL fitting-program. These extinction values have a very important uncertainty due to the limited wavelength range (optical) of our spectroscopic observations, which prevents minimizing degeneracies with age, metallicity, and star formation history. In Fig. 2 we summarize these estimates. In general, the gas dust attenuation has a mean value of ~ 1.5 magnitude, that is in agreement for what is found for other spiral galaxies [8]. We find that the gas attenuation appears larger than the continuum attenuation as already know from [3], and we find $\langle E(B - V)_{\text{continuum}} \rangle \sim 0.3 \times \langle E(B - V)_{\text{ionized-gas}} \rangle$. This is somewhat expected given that, as shown in [5, 20], in nearby spiral galaxies stars, gas and dust are decoupled and the attenuation inferred from the $\text{H}\alpha/\text{H}\beta$ ratio is typically higher than that inferred from the spectral continuum (e.g., [3, 4]). Recently, [16] and [15] explain this result as selective

dust extinction because a large fraction, but not all, of the dust in galaxies is associated with star formation regions, absorbing a significant fraction of the light emitted by the young stars.

5.2 Metallicity

We also estimate oxygen abundances and, in order to quantify the abundance gradient, we have carried out three linear regression fits to the data. The first one is a fit for all points weighted by own errors ($\chi_{red}^2 = 1.45$). The gradient in this case has a value of $-0.035 \text{ dex kpc}^{-1}$ ($-0.0042 \text{ dex arcsec}^{-1}$) in agreement with the uncertainties derived for the rings showed in grey zone. The oxygen abundances varies, according to the adopted diagnostic, between $12 + \log(\text{O}/\text{H}) = 8.15$ and $12 + \log(\text{O}/\text{H}) = 8.7$ (i.e. from approximately 1/3 the solar oxygen abundance to nearly the solar value). The second and the third fits are double fits on the data with a free parameter, the radius of break, where one is weighted by the data errors, (black solid line) and the other is unweighted, (for both $\chi_{red}^2 = 0.55$). We find as a main result that, while the O/H ratio follows the radial gradient known from previous investigations in inwards zone ($12 + \log(\text{O}/\text{H})_{r=0} = 8.9$ and a gradient value of $-0.140 \pm 0.016 \text{ dex kpc}^{-1}$) the outer abundance trend, from a radius of $35.8''$ ($\sim 4.4 \text{ kpc}$) flattens out to an approximately constant value of $12 + \log(\text{O}/\text{H})_{r=0} = 8.27$ with a gradient of $0.002 \pm 0.019 \text{ dex kpc}^{-1}$ and even reverses. This result might be interpreted in the context of the effects of stellar migration or it could implies different star formation histories between the inner and outer parts of the disk of this galaxy [2]. The change in the slope of the metallicity gradient (and the steep inner color gradients) can be interpreted as due to mixing induced by a bar or probably due to stellar diffusion. An abrupt discontinuity in the radial oxygen abundance trend is also detected near the optical edge of the disk. Figure 3 shows the metallicity derived in our HII regions sample using the Kewley & Dopita recipe. From the theoretical side, a negative gradient (in logarithmic abundance) can be reproduced by *inside-out* scenarios of galaxy formation in which the timescale for the formation of the disk increases with galactocentric distance [1]. The change in the slope of the metallicity gradient (and the steep inner color gradients) can be interpreted as due to mixing induced by a bar while the reddening of the outer color profiles seems more likely related with stellar diffusion.

6 Conclusions

We investigated the properties of 73 individual HII regions in NGC 5668 using integral field spectroscopy technique. To improve our knowledge on radial variation of the main properties of star and gas, we also selected 18 concentric annuli in this galaxy and finally we analyze spectra that cover almost the entire spectral range from 3700 to 6700 Å. We use those data to estimate the attenuation (from the $\text{H}\alpha/\text{H}\beta$ Balmer decrement) and find that the dust attenuation has a mean value of ~ 1.5 magnitude, almost a factor of three difference with continuum extinction. We study the chemical abundance traced by the oxygen (using strong-line methods such as the R_{23} ; [9]) and we find a negative gradient of $-0.035 \text{ dex kpc}^{-1}$ that flattens in the outer zone ($R_{\text{break}} \sim 4.4 \text{ kpc}$).

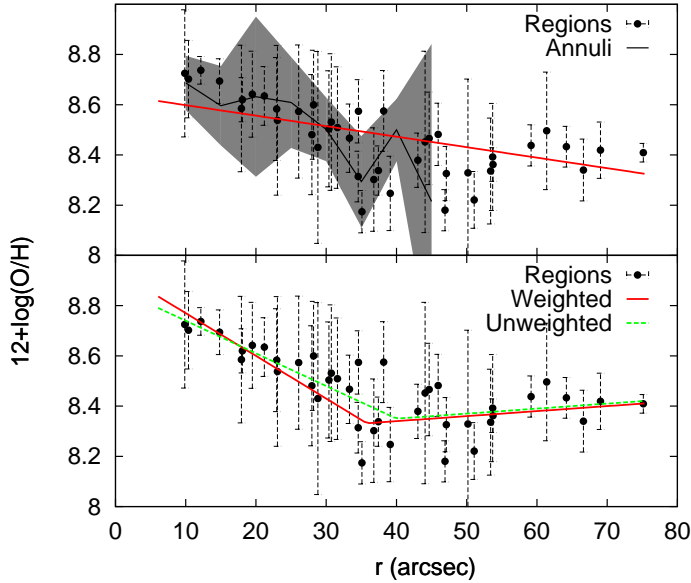


Figure 3: Radial abundance gradient in NGC 5668, where black filled-circles correspond to individual HII regions while the black line represents the values obtained for the concentric annuli and coloured lines represents the fits done. *Top panel:* The grey zone represents the error's bars for the solid line and the red line symbolize the linear regression fit to the data points for the HII regions. We obtained a gradient of $-0.035 \text{ dex kpc}^{-1}$. *Bottom panel:* We draw two types of fit: red line reproduce a double fit weighted by own data errors. The slope of the gradient is $\sim -0.140 \text{ dex kpc}^{-1}$ for inner part and $0.002 \text{ dex kpc}^{-1}$ for outer part. Green dashed line reproduce unweighted double fit with values of $-0.1073 \text{ dex kpc}^{-1}$ (inner) and $0.002 \text{ dex kpc}^{-1}$ (outer) for the gradient.

References

- [1] Boissier, S., & Prantzos, N. 1999, MNRAS, 307, 857
- [2] Bresolin, F., et al. 2009, ApJ, 700, 309
- [3] Calzetti, D., et al. 1994, ApJ, 429, 582
- [4] Calzetti, D., et al. 1996, ApJ, 458, 132
- [5] Calzetti, D., et al. 2000, ApJ, 533, 682
- [6] Garnett, D., 1992, ApJ, 103, 1330
- [7] Gil de Paz, A., & Madore, B. F. 2002, NOAO
- [8] Gil de Paz, A., et al. 2007, ApJ, 561, 115
- [9] Kewley, L., & Dopita, M. 2002, ApJ, 142, 35

- [10] McCall, M., et al. 1984, *ApJ*, 57, 1
- [11] Nakano, S., et al. 2004, *IAUC*, 8272, 1N
- [12] Osterbrock, D. E. 1989, *University Science Books*
- [13] Pagel, B. E. J., et al. 1992, *MNRAS*, 255, 325
- [14] Pohlen, M., & Trujillo, I. 2006, *A&A*, 454, 759
- [15] Poggianti, B. M., & Wu, H. 2000, *ApJ*, 529, 157
- [16] Poggianti, B. M., et al. 1999, *ApJ*, 518, 576
- [17] Roskar, R., et al. 2008, *ApJ*, 65, 68
- [18] Sánchez, S. F., et al. 2006, *MNRAS*
- [19] Schulman, E., et al. 1996 *AAS*, 189, 608
- [20] Stasińska, G., et al. 2001, *A&A*, 374, 919